Trop J Nat Prod Res, September 2023; 7(9):3936-3943 **ISSN 2616-0684 (Print)**
ISSN 2616-0692 (Electronic)

Tropical Journal of Natural Product Research

Available online at https://www.tjnpr.org

Original Research Article

The Toxic Impact of Silver Nanoparticles Synthesized Extracellularly by *Aspergillus flavus* on Breast Cancer Cells (MDA-MB-231), as Well as Their Antibacterial Activity

Ibrahim I. Alfarrayeh[1,*]; Safa S. Al-Alwani[2]; Yaseen T. Al Qaisi[3]; Ahmad Z. Alsarayreh[3]; Laila Al-Omari [4]; Jehad F. Alhmoud[4]; Moath Alqaraleh[1]

[1]*Department of Applied Biology, Faculty of Science, Tafila Technical University, 66110, Tafila, Jordan.*
[2]*Faculty of Allied Medical Sciences, Al-Ahliyya Amman University, 19328, Amman, Jordan.*
[3]*Department of Biological Sciences, Faculty of Science, Mutah University, 61710, Al-Karak, Jordan.*
[4]*Department of Medical Laboratory Sciences, Jordan University of Science and Technology, P.O. Box 3030, Irbid, 22110, Jordan.*

ARTICLE INFO

Article history:
Received 13 June 2023
Revised 20 August 2023
Accepted 25 September 2023
Published online 01 October 2023

ABSTRACT

Silver nanoparticles (AgNPs), with unique properties and diverse uses from antimicrobials to drug carriers, have gained prominence. This study examined the anti-cancer and anti-bacterial properties of biogenic AgNPs produced from the filtrate of *Aspergillus flavus*. AgNPs (0–200 µg/mL) were assessed against fibroblasts and breast cancer cell lines (MDA-MB-231). AgNPs were antiproliferative to MDA-MB-231 cells at 6 µg/mL and above but cytotoxic to fibroblasts at 12 µg/mL and beyond. MDA-MB-231 cells were treated to the marginally effective concentration of AgNPs, 3 µg/mL, in order to evaluate gene regulation. However, there was a significant downregulation of cyclin D1 and BCL-2. Nevertheless, MDA-MB-231 cells treated with 3 µg/mL AgNPs exhibited a significant increase in the pro-apoptotic caspase 3 genotype. After MDA-MB-231 cells were subjected to 3 µg/mL AgNPs, the pro-inflammatory cytokines IL-1β and IL-6 were significantly downregulated. At 3 µg/mL, AgNPs raised TNF-α, an anti-inflammatory cytokine. AgNPs exhibited substantial antibacterial efficacy against all examined bacterial strains through the implementation of the disc diffusion methodology. However, the MIC data for AgNPs' antibacterial activity showed that *Salmonella enterica*, *Salmonella typhi*, *Staphylococcus epidermidis*, and *Staphylococcus aureus* were the highest influenced stains, with Minimum Inhibitory Concentration (MIC) value of 6.38 µg/mL, whereas *Escherichia coli* ATCC 25922, *Pseudomonas aeruginosa*, and *Escherichia coli* ATCC 10145 had MIC value of 19.15 µg/mL. In conclusion, AgNPs from *A. flavus* have potential antibacterial effects against various pathogens and showed cytotoxicity against MDA-MB-231 breast cancer cells, indicating wide-ranging biological relevance.

Keywords: Nanoparticles; *Aspergillus flavus*; Cytotoxicity; Antibacterial; Anticancer

Introduction

Silver nanoparticles (AgNPs) have exhibited significant efficacy in suppressing the proliferation of diverse pathogenic microorganisms. Due to their robust antimicrobial characteristics, they have become highly prized resources in various biotechnology domains. The production of AgNPs can be accomplished through various means, including physical, chemical, and biological processes. Each approach has its own set of benefits and drawbacks.[1,2] A comprehensive comprehension of techniques for synthesizing AgNPs was achieved through an extensive literature review, which involved an in-depth analysis of the vast array of scholarly research available on the subject matter. AgNPs have been identified as a reliable and effective remedy for various prevalent issues, such as antiviral, antibacterial, anticancer, dental applications, bone healing, and bone cementing.

*Corresponding author. E mail: Alfarrayeh@gmail.com
Tel: 00962790632435

Citation: Alfarrayeh II, Al-Alwani SS, Al Qais YT, Alsarayreh AZ, Al-Omari L, Alhmoud JF, Alqaraleh M. The Toxic Impact of Silver Nanoparticles Synthesized Extracellularly by *Aspergillus flavus* on Breast Cancer Cells (MDA-MB-231), as Well as Their Antibacterial Activity. Trop J Nat Prod Res. 2023; 7(9):3936-3943 http://www.doi.org/10.26538/tjnpr/v7i9.14

Official Journal of Natural Product Research Group, Faculty of Pharmacy, University of Benin, Benin City, Nigeria

The inherent antibacterial, antiviral, and anticancer characteristics of multifaceted nanoparticles have led to their application in various biological contexts.[3]

The biosynthesis of AgNPs utilizing biomolecules such as enzymes/proteins, amino acids, carbohydrates, and vitamins has emerged as a simple, effective, economical, and environmentally friendly approach. This method leverages the properties of bacteria, fungi, as well as plant extracts, and small biomolecules like amino acids and vitamins.[2,4,5] Interestingly, certain AgNPs have exhibited exceptional efficacy against diverse bacteria species that have developed high levels of resistance to conventional pharmaceuticals.[6,7] Furthermore, nanoparticles have demonstrated their potential as carriers for delivering antimicrobial medications to infected organs within the body, capitalizing on their incredibly small size.[8,9] It is plausible that these biogenic nanoparticles may serve as viable alternatives to existing medications, which bacteria have evolved resistance against.

In addition to their biomedical applications, these non-toxic nanoparticles offer a promising solution to address the issue of microbial contamination in drinking water.[10] Every year, millions of individuals, particularly in developing nations, suffer from waterborne diseases caused by microbial contaminants. In this regard, AgNPs have shown remarkable potential as an effective water disinfectant, enabling the provision of clean and safe drinking water, free from harmful microbes, and suitable for human consumption. By harnessing the disinfecting capabilities of these nanoparticles, we have the opportunity to make a significant impact on global public health.[2,10,11]

AgNPs have also demonstrated promising anticancer activity, making them a subject of intense research in the field of oncology.[12,13] AgNPs exhibit selective cytotoxicity towards cancer cells while sparing normal cells, which is attributed to their unique physicochemical properties.[14,15] These nanoparticles have been shown to induce apoptosis, inhibit cell proliferation, and interfere with angiogenesis, thus hampering tumor growth. Moreover, AgNPs possess the ability to target and penetrate cancer cells due to their small size and surface charge, leading to increased accumulation and drug delivery within the tumor microenvironment.[12]

Although substantial progress has been made in researching the anticancer and antibacterial activities of AgNPs, there are still gaps in our understanding and areas that require further exploration. Given the immense potential of AgNPs as therapeutic agents against cancer and drug-resistant bacteria, it is crucial to conduct additional investigations to fully comprehend their capabilities and enhance their effectiveness. In this study, our objective was to examine the anti-cancer and antibacterial properties of biogenic AgNPs synthesized using *Aspergillus flavus*.

Materials and Methods

Bacterial strains and reagents

Sigma-Aldrich supplied all of the chemicals and media used. The organisms used in the antibacterial assay were Gram-positive and Gram-negative. All of these strains were collected from the Karak Government Hospital (KGH) and identified using a Highly Automated System for Identification and Antimicrobial Susceptibility Testing (BIOM'RIEUX) such as VITEK® 2 Compact. The strains of bacteria were kept alive by subculturing them on nutrient agar regularly and keeping them at 4℃ before use. All solutions were prepared with deionized water of the highest purity.[16]

Generation of AgNPs by Aspergillus flavus and its characteristics

The presence of *A. flavus*, a species of fungus, was detected in the supply warehouses located on the campus of the University of Mutah in Jordan, as concluded by the investigation conducted by Al-Soub *et al*.[6] For the screening of AgNPs, the methodology described by Gurunathan *et al*[17] was employed. In brief, the fungal isolates were cultivated aerobically at 37°C for varying periods in suitable media. Subsequently, the cells were suspended in a sterile medium and centrifuged at 10,000 rpm for 20 minutes to obtain a fungal extract. Following centrifugation, the supernatant was mixed with 1 mM silver nitrate in a 1:1 ratio, and the pH of the reaction mixture was adjusted to 8.5. The resulting mixtures were then agitated at 37°C in the dark, with shaking at 200 rpm, until a transition from pale yellow to dark brown coloration occurred. The initial color change from bright yellow to brown was used as an indicator for the formulation and was further verified through UV-Vis spectroscopy. To examine the size and dispersion of the nanoparticles, a Transmission Electron Microscope (TEM) was utilized.[6,18] Further characterizations of the AgNPs properties, including morphology, Zeta potential, Zeta sizer, FT-IR, and XRD analyses, were performed and documented in our previously published article by Al-Soub *et al*.[6]

Cancer cell lines culture

Humans' breast cancer cell line MDA-MB-231 (ATCC HTB-26) and human periodontal ligaments fibroblasts cell lines (PDL) were employed. All of the cell lines were propagated in DMEM with 10% fetal bovine serum (FBS), 10 mM HEPES Buffers, 100 µg/L L-Glutamines, 50 µg/L Gentamicin, 100 µg/L Penicillin, and 100 mg/L Streptomycin in a humidified 5% CO_2 incubator at 37°C.

Cytotoxicity assay

Every cell was grown in a humidified, 37°C, 5% CO_2 incubator. First, 75 mL flasks containing all the cells were rinsed with 3-5 mL of phosphate buffer saline (PBS), and then 1-2 mL of trypsin were added until the cells detached. Each cell line received an equal amount of fresh medium, which was then gently pipetted to break up any clumps and guarantee a consistent single-cell suspension. Harvesting and counting of cells for each cell line, the frequency and ratio of cell propagation were anticipated. Once the appropriate number of cells had been reached, the cells were propagated every two to three days. When counting cells, 100 µL of 4% (w/v) trypan blue dye was combined with 25 µL of the extracted cells. The cell suspension was then placed at the edge of a hemocytometer counting chamber.[19,20]

The cytotoxicity was evaluated by using the MDA-MB-231 cell line which was obtained from the research lab at the Pharmacological and Diagnostic Research Center, Faculty of Pharmacy, Al-Ahliyya Amman University, Amman, Jordan. Cell toxicity was measured after exposure to AgNPs (3-200 µg/mL). After 24 hours of incubation at 37 °C in DMEM at a cell density of 1×10^4 per well, the cells were split into fresh DMEM with varying concentrations of AgNPs for an additional 48 hours. To conduct the MTT experiment, we first withdrew the media from the wells and then incubated the cells for 4 hours at 37 °C in 20 µL of MTT solution (5 mg/ml). After discarding the MTT solution, insoluble formazan crystals were dissolved by adding 200 µL of dimethyl sulfoxide (DMSO). At 570 nm and 630 nm, optical density was determined. Information was collected from three independent wells. Primary cell cultures of human periodontal ligament fibroblasts (PDL) (which were also obtained from the research lab at the Pharmacological and Diagnostic Research Center, Faculty of Pharmacy, Al-Ahliyya Amman University, Amman, Jordan) were used to confirm the selective cytotoxicity. Assays were run in triplicate, and the IC50 antiproliferative activities were presented as the means standard deviations (n=3).[20]

Gene expression level assay

MDA-MB-231 cell line was plated at a density of 1×10^6 cells/well in 6-well plates.[21] The genes for IL-6, IL-1β, TNF-α, Cyclin D1, BCL-2, and caspase-3 After 24 hours of incubation with the selected concentrations of AgNPs, fold changes were calculated.[22]

Ribonucleic Acid (RNA) Extraction and Analysis

RNeasy Mini kit was used to isolate total RNA (QIAGEN, USA). Cell pellets were removed from -80°C storages, defrosted on ice, and then resuspended in 500 µL 2-mercaptoethanol-containing lysis solutions. To remove cellular debris, 500 µL of 70% ethanol solution was added to the lysate filtrate and vortexed thoroughly. Next, the cell lysates were transferred to RNeasy Mini spin columns and spun for 15 seconds at 10,000 revolutions per minute. A binding column held captured RNA molecules in their whole. After the flow-through liquids had been discharged, the collecting tubes were returned to a binder column. The wash process was repeated thrice. After then, a new collecting tube was employed to contain the binding columns. To extract the RNA, 50 µL of RNase-free water was poured directly into the membranes of the spin columns and centrifuged for one minute at 10,000 rpm. Refined RNA was instantly collected and kept at -80°C. Using Nanodrop ND-1000 spectrophotometers, the concentrations and purity of recovered total RNA were evaluated (Thermo Scientific, Wilmington, USA). 260 nm and 280 nm optical densities were calculated. For the vast majority of RNA-isolated samples, the ratio (A260/A280) fell between 1.8 and 2.1.[2,23]

Complementary Deoxyribonucleic Acid (cDNA) synthesis

cDNA was produced using a reverse transcription process (Applied Biosystem, USA). Two micrograms of total RNA and 1 µl of oligodeoxythimidine primers were added to a microcentrifuge tube and heated for five minutes at 65 °C on a thermocycler C 1000 (Bio-Rad, USA). They were immediately centrifuged and placed on ice. The 20 µl reaction solution was made using the following chemicals: 1.4 µl of 25 mM $MgCl_2$ and 4 µl of a mixture of 10 mM dNTPs. Avian myeloblastosis virus reverse transcriptase (1 µL), recombinant RNasin® ribonuclease inhibitor (1 µL), reversed transcriptase 10x buffers (2 µL) (AMV-RT). The temperature requirements for cDNA synthesis were as follows: Microcentrifuge tubes were incubated at 37°C for thirty minutes. To denature the RNA template and inactivate proteins, the reaction mixture was initially heated for five minutes at 95°C. Following a 5-minute incubation time at 4°C, microcentrifuge tubes were stored at -80°C for further analysis. The concentration and purity of cDNA were determined using a Nanodrop ND-1000 spectrophotometer. The absorbance readings were taken at 260 nm and 280 nm, and the A260/A280 ratio was calculated. The majority of the recovered cDNA specimens exhibited A260/A280 ratios between 1.6 and 1.8, indicating good purity.[24]

Table 1: List of primer sequences used for selected genes.

Gene name or symbol	Primer sequence	References
Cyclin D1	Forward: 5'-ACC TGA GGA GCC CCA ACA A-3'	[49]
	Reverse: 5'-TCT GCT CCT GGC AGG CC-3'	
IL-6	Forward: 5′-GGTACATCCTCGACGGCATCT-3′	[21]
	Reverse: 5′-GT GCCTCTTTGCTGCTTTCAC-3′	
IL- 1β	Forward: 5'- ATGGCAACTGTTCCTGAACTCAAC -3'	[21]
	Reverse: 5'- CAGGACAGGTATAGATTCTTTCCTTT -3'	
TNF-α	Forward: 5'- ATGAGCACAGAAAGCATGATCCG -3'	[21]
	Reverse: 5'- TCACAGAGCAATGACTCCAAAGTAG -3'	
BCL-2	Forward: 5'-AAG CCG GCG ACG ACT TCT-3′	[50]
	Reverse: 5'-GGT GCC GGT TCA GGT ACT-3′	
caspase-3	Forward: 5′-AGCAAACCTCAGGGAAACATT-3′	[50,51]
	Reverse: 5′-CTCAGAAGCACACAAACAAAACT-3′	

Relative Quantitative RT-PCR Analysis

For relative-quantitative analyses of mRNA expression rates of the studied enzyme, quick SYBR green kappa master mixes were utilized (Biosystem, USA). In each PCR reaction, 200 nM of the forward and reverse primers were combined with 1x KAPA SYBR greens quick masters' solution, 1-2 L of cDNA templates, and a final volume of 20 L. The primer combination sequences utilized are listed in Table 1. For the PCR amplifications, the IQ5 multicolor real-time PCR detection system (Bio-Rad, USA) was utilized. Every method resulted in melting curves between 70 and 95℃. As an internal reference gene, glyceraldehyde-3-phosphates dehydrogenase (GAPDH) was used to normalize the expressions of the studied genes. The efficiency of the PCR reaction was tested utilizing the approach of calibrating curves for quantitatively comparable data. Pffafl was used to determine the data for the expression level of mRNA.[25]

$$RQ = \frac{(E_{target})^{\Delta Ct\,(target)}}{(E_{reference})^{\Delta Ct\,(reference)}}$$

Whereby

$$\Delta Ct(target) = Ct(target\ gene\ in\ calibrator) - Ct(target\ gene\ in\ test)$$

$$\Delta Ct(reference) = Ct(reference\ gene\ in\ calibrator) - Ct(reference\ gene\ in\ tests)$$

and the amplification efficiency was calculated using the following formula:

$$E = 10^{-1/slope}$$

In one instance, the effectiveness was 2 (the effectiveness of both the targets and references genes is equal to 2), and the slopes were -3.32 if the number of references and targeted DNA areas are doubling each cycle which is calculable assuming:

$$RQ = \frac{2^{\Delta Ct(target)}}{2^{\Delta Ct\,(reference)}}$$

$$= 2^{[\Delta Ct(target) - \Delta Ct(reference)]}$$

$$= 2^{[(Ct(target,calibrator) - Ct(target,test)] - [(Ct(ref,calibrator) - Ct(ref,test)]}$$

$$= 2^{-[(Ct(target,test) - Ct(target,calibrator)] - [(Ct(ref,test) - Ct(ref,calibrator)]}$$

$$= 2^{-\Delta\Delta Ct}$$

The results were obtained from three independently performed experiments.

Antibacterial activity of AgNPs

Gram-positive bacteria (*Staphylococcus epidermidis* and *Staphylococcus aureus*) and Gram-negative bacteria (*Pseudomonas aeruginosa*, *Escherichia coli*, *Pseudomonas aeruginosa* (ATCC 10145), *Escherichia coli* (ATCC 25922), *Salmonella enterica* (ATCC 13076), and *Salmonella typhi* (ATCC 14028)) were tested against the biosynthesized AgNPs. All of the bacterial strains were stored on MH agar until needed. The Kirby-Bauer disc diffusion susceptibility test was used to assess the antibacterial activity of AgNPs against pathogenic microorganisms. Bacteria were spread on Mueller-Hinton agar (MHA) using sterilized cotton swabs (Merck, Germany). The sterilized disc (6 mm) contained AgNPs (5 µg/disc), or a negative control (DMSO). After 24 hours at 37°C, the plates were removed and the inhibitory zone diameter measured in millimeters. Each sample underwent three independent tests.[5,16,19,26]

MIC determination

The broth microdilution method established by the Clinical Laboratory Standards Institute was used to calculate AgNPs' MIC, which is the lowest concentration at which no bacterial growth is detected (Wayne and Clinical and Laboratory Standards Institute 2012). In duplicate, 96 well microtiter plates were used to culture bacteria in nutritional broth. 5×10^5 CFU ml-1 was the final bacterial concentration in each microtitre plate well. AgNPs from 0.016 to 1024 µg/mL were tested on various microorganisms. The experiment included two controls: a sterile broth and a broth with bacterial inoculum. Bacterial microtitre plates were incubated at 37 °C for 24 hours. After that, manual calculation estimated MIC values.[27–29]

Statistical analysis

Using the non-parametric Mann-Whitney test, any significant group differences were determined. In addition, Dunnett's post hoc test was utilized following a one-way analysis of variance (ANOVA) for normally distributed data. The analysis of the data with SPSS 22 (SPSS, Inc., USA). The remaining results were presented as the means and standard deviations (SD) of three to four independent experiments. After doing an ANOVA in GraphPad Prism, Dunnett's post hoc test was utilized to analyze the statistical differences between the control and treatment groups. In all statistical studies, a p-value less than 0.05 was regarded as statistically significant. If the p-value was less than 0.001, a statistical difference was considered to be very significant.[30]

Results and Discussion

Silver nanoparticles (AgNPs) biosynthesis

The airborne fungus was initially isolated from the warehouses of the Supplies and has been identified as *A. flavus*, according to the findings of the investigation. A dark brown color was formed when the fungal filtrate was incubated with silver nitrate ($AgNO_3$), whereas control samples stayed constant during the 24-120 hours' incubation period (Figure 1a). UV-vis absorption spectra (UV-vis) of the fungal filtrate were measured (Figure 1b). The UV-vis spectrum as in Figure 1b shows the peak of SPR for AgNPs at 427 nm. The AgNPs were discovered to be reliable in their native form, with no detectable

modifications. The TEM pictures (Figures 2a and 2b) demonstrate that the tested particles are made up of a variety of tiny objects, each smaller than 0.5 m in size. The nanoparticles seen in the TEM image are typically less than 35 nm in size and are almost spherical.

The filtrate derived from *A. flavus* biomass proficiently facilitated the synthesis of AgNPs from $AgNO_3$, evident through a noticeable transition in color from a pale yellow shade to a deep brown hue. Our research team previously scrutinized the attributes of AgNPs biogenetically generated through *A. flavus* extracellular filtrate, employing techniques encompassing UV-Vis spectrophotometry, zeta sizer, FTIR, and transmission electron microscopy (TEM).[6] According to FTIR analysis, bioactive functional groups of AgNPs which can be derived from biomolecules such as proteins, enzymes, or hydrocarbons, can interact with the surface of AgNPs and impact their stability, reactivity, and interactions with biological systems. The effects of bioactive functional groups on AgNPs' bioactivities include stabilization, biocompatibility, targeting, cellular interactions, biological activity, and toxicity and safety.[2,31]

AgNPs cytotoxic activity study

Various concentrations of the bio-fabricated AgNPs, including 3, 6, 12, 25, 50, 100, and 200 µg/mL, were evaluated against a fibroblast cell line that served as a control and an MDA-MB-231 cell line (Figures 3 and 4). There was a decrease in the cell viability of fibroblast cell lines that had been exposed to AgNPs at concentrations of 12 µg/mL or higher. However, a concentration-dependent inhibition took place, and it was determined that these cells reached a 40% reduction in viability when exposed to 200 µg/mL of AgNPs. Fibroblast cells were not significantly affected by the presence of 3 and 6 µg/mL of AgNPs. In contrast, all concentrations of AgNPs led to a significant decrease in the cell viability of MDA-MB-231, with the exception of a concentration of 3 µg/mL, which led to a fall in cell viability of 20%. This was the only concentration that did not lead to a loss in cell viability. The value for the IC50 was determined to be 37.75 µg m-1 (Figure 3). As a consequence of this, the MDA-MB-231 cell lines were subjected to additional testing for the purpose of researching gene expression. The findings of this research indicated that the air-born *A. flavus* cell filtrate had the ability to create AgNPs that possessed antibacterial, anti-inflammatory, and anticancer potential.

Effect of AgNPs on Expression of Genes in MDA-MB-231 Cells

Pro- and Anti-Apoptotic genes

MDA-MB-231 cells were used in this study to investigate the impact of AgNPs on the expression of pro- and anti-apoptotic genes (Figure 5). MDA-MB-231 cells were treated with AgNPs at a concentration of 3 µg/mL for 24 hours. In the MDA-MB-231 cell line that was subjected to different concentrations of AgNPs, the effect of 3 µg/mL of AgNPs showed that there was a statistically significant elevation of caspase 3, the pro-apoptotic genotype. This was in comparison to cells that had not been treated. The findings suggest that anti-apoptotic genes, such as BCL-2 and cyclin D1, have been deregulated to some degree. Our investigations with caspase-3 showed that apoptosis might be triggered in MDA-MB-231 cancer cells by the presence of AgNPs.

Expression of IL-beta, IL-6, and TNF-α

The treatment of MDA-MB-231 cells with AgNPs resulted in lower levels of IL-1β and IL-6 while simultaneously increasing levels of TNF-α (Figure 5). When compared to untreated cells, the pro-inflammatory cytokines IL-1β and IL-6 were significantly downregulated in the MDA-MB-231 cell line after exposure to AgNPs at a concentration of 3 µg/ml. In addition, the anti-inflammatory cytokine TNF-α was considerably increased when the AgNPs were present at a concentration of 3µg/mL.

Toxicological studies describing cell responses to harmful chemicals require the cell viability assay, which can reveal details about the metabolic activity, cell death, and survival.[32] Both the MDA-MB-231 cell and the fibroblast cell lines were tested with AgNPs at a variety of dosages (0-200 µg/mL) for 24 hours, and the results point out that AgNPs were capable of lessening the MDA-MB-231 cells viability on a dose-reliant way. Concentrations of 12 µg/mL or higher of AgNPs were required to cause cytotoxicity in fibroblasts; whereas, concentrations of 6 µg/mL or higher caused antiproliferative effects in MDA-MB-231 cells. Fungi may biosynthesize nanoparticles quickly and efficiently; these particles might be more cytotoxic to cancer cells than to fibroblasts. Our results were in line with a prior work by Gurunathan *et al*.[33] which demonstrated that AgNPs had stronger cytotoxicity than $AgNO_3$ and showed dose-dependent cytotoxicity in human Chang liver cells. Depending on the kind of cell and the size of the nanoparticles utilized, the amount of metabolic activity in cells treated with AgNPs was decreased.[34] There is evidence that colloidal silver has a dose-dependent cytotoxic effect on MDA-MB-231 breast cancer cells.[35]

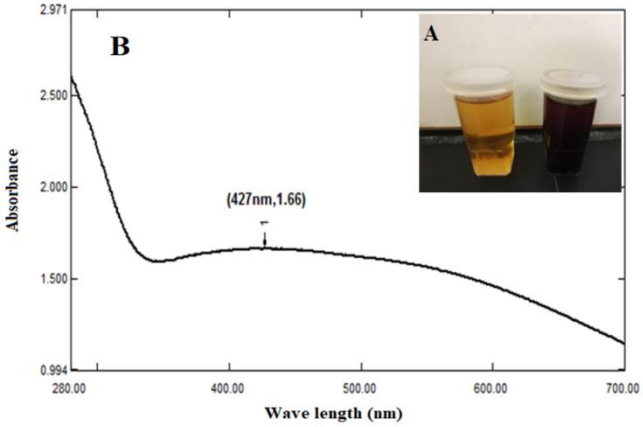

Figure 1: After optimization, biosynthesis of AgNPs utilizing 1 mM $AgNO_3$ and filtrate devoid of fungal biomass. (A) color alteration, and (B) UV-Visible spectra

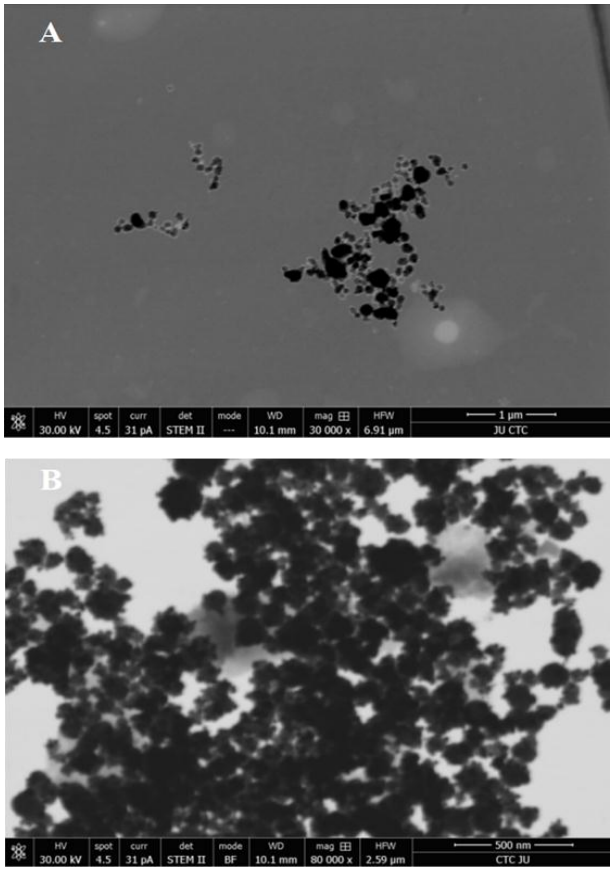

Figure 2: TEM Image of biosynthesized AgNPs. Magnification (A) 30,000x, (B) 80,000x

Table 2: Antibacterial activity of AgNPs synthesized by *A. flavus* filtrate as measured by Inhibition Zones (mm) and Minimum Inhibitory Concentration (µg/mL).

Bacteria	AgNPs Inhibition zone (mm)	MIC (µg/mL)
Salmonella enterica (ATCC 13076)	17.5 ± 0.5	6.38
S. typhi (ATCC 14028)	15.5 ± 0.5	6.38
S. aureus	18.5 ± 0.5	6.38
E. coli	14.0 ± 0.0	19.15
E. coli ATCC 25922	13.5 ± 0.6	19.15
S. epidermidis	17.5+0.7	6.38
P. aeruginosa	12.5 ± 0.5	19.15
P. aeruginosa ATCC 10145	12.3 ± 0.3	19.15

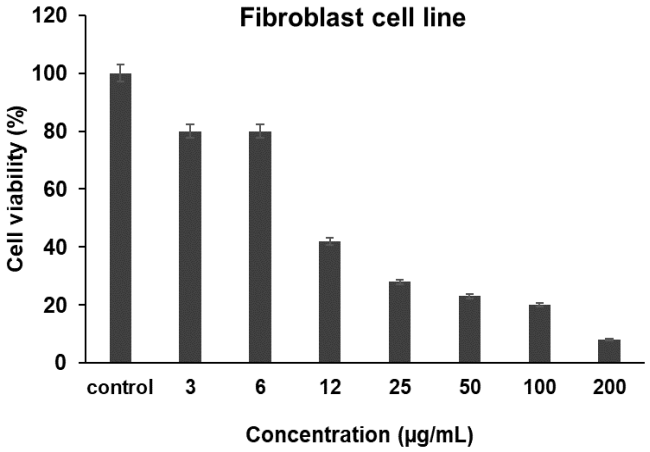

Figure 3: The antiproliferative activity of AgNPs on the Fibroblast cell line based on MTT assay. The result represents the percentage of cell viability under different concentrations of AgNPs.

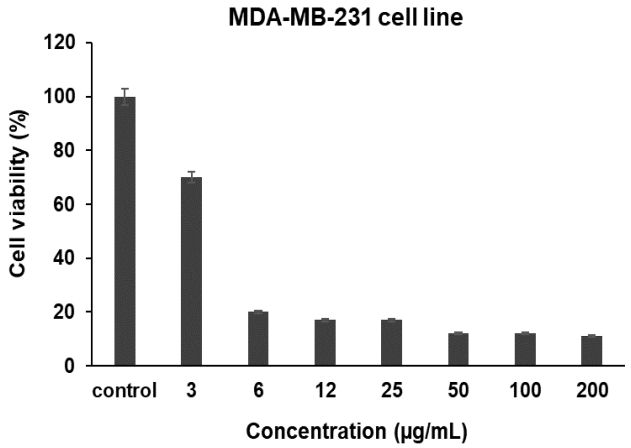

Figure 4: The antiproliferative activity of AgNPs on the MDA-MB-231 cell line based on MTT assay. The result represents the percentage of cell viability under different concentrations of AgNPs.

In addition, the MDA-MB-231s were exposed to 3 µg/mL of AgNPs to examine the treatment's effects on gene regulation. The MTT experiment demonstrated the cytotoxicity of AgNPs against the MDA-MB-231 cells in a dose-related fashion. This confirmed the significant anticancer activity of the nanoparticles at low doses. On the other hand, it was shown that anti-apoptotic genes including cyclin D1 and BCL-2 had undergone several folds of downregulation. We looked into the potential impact that AgNP might have on the apoptotic pathway by measuring the activity of caspase-3 in MDA-MB-231 cells after treatment with AgNP. The MDA-MB-231 cell line was exposed to different doses of AgNPs, and the effect of 3µg/mL AgNPs revealed that caspase 3, a genotype linked to pro-apoptotic behavior, was markedly elevated. The activation of caspase-3 has been demonstrated to be a key component of numerous apoptotic pathways.[36] This rise in caspase-3 activity, which was achieved by utilizing 3µg/mL AgNPs, demonstrates that a considerably lower concentration of AgNPs than 3µg/mL AgNPs is required to activate caspase-3.[33] Given that the AgNPs appear to have an effect on cellular metabolic activity, the likelihood of apoptosis stimulation by the AgNPs was investigated, particularly at concentrations of 3 µg/mL of AgNPs or lower. Caspase 3 activation at high levels provided obvious evidence that AgNPs were responsible for the cells' apoptotic demise. The administration of AgNPs results in a decrease in both IL-1 and IL-6 levels while increasing TNF-α. TNF-α, a key therapeutic target in several chronic inflammatory disorders,[37,38] also links inflammation and cancer and appears to be a critical mediator in this association.[39] Other investigations have demonstrated that particular bioactive substances can have an effect on several anti-apoptotic genes, hence preventing these genes from performing their immediate protective function against apoptosis and leading to the death of apoptotic cells.[40–42]

AgNPs antibacterial activity study

The disc diffusion method

According to the findings, there was a significant antibacterial activity of AgNPs towards all of the bacteria that were used. When tested against Gram-positive bacteria, AgNPs showed inhibition zones of 18.5±0.5 and 17.5±0.7 mm, respectively, for *S. aureus* and *S. epidermidis*. In contrast, the inhibition zones for *Salmonella enterica*, *E. coli*, *E. coli ATCC 25922*, *P. aeruginosa*, and *P. aeruginosa* ATCC 10145 were 17.5±0.5 mm, 14.0±0.0 mm, 13.5±0.6 mm, 12.5±0.5 mm, and 12.3±0.3 mm, respectively (Table 2).

Minimal Inhibitory Concentration

The outcomes of an examination into the antibacterial activity of AgNPs that made use of the microdilution method are presented in Table 2. Five distinct types of Gram-negative bacteria and two distinct types of Gram-positive bacteria were used in this experiment.

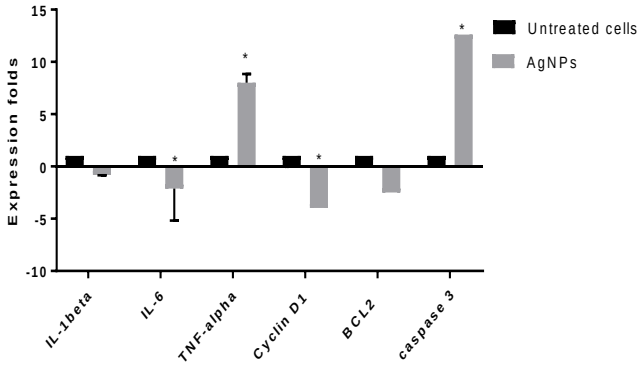

Figure 5: Effect of AgNPs on the expression of caspase 3, BCL2, and Cyclin D1 in MDA-MB-231 cell line, cells were treated with 3 µg/mL of AgNPs. The results were expressed as a mean of three dependent replicates ± SD. *: $p<0.05$, compared to control untreated cells.

Salmonella enterica, *S. typhi*, *S. aureus*, and *S. epidermidis* were the most affected stains, which resulted in a MIC of 6.38 µg/mL. In contrast, the minimum inhibitory concentration (MIC) for E. coli ATCC 25922, *P. aeruginosa*, *E. coli*, and *P. aeruginosa* ATCC 10145 was found to be 19.15 µg/mL.

The findings of this study demonstrated that AgNPs are extremely effective against every type of bacterium that was tested. AgNPs exhibited a variety of inhibitory zones when tested against Gram-positive and negative bacteria. These zones ranged in size from 12.3 mm for *P. aeruginosa* ATCC 10145 to 18.5 mm for S. aureus. However, the MIC data for the antibacterial activity of AgNPs showed that *Salmonella enterica*, *S. typhi*, *S. aureus*, and *S. epidermidis* were the most impacted stains, with MICs of 6.38 µg/mL, while the MIC for the two *E. coli* strains and both *P. aeruginosa* strains were 19.15 µg/mL. It was shown that AgNPs' antibacterial activity differed among Gram-positive and Gram-negative bacteria. AgNPs are effective against Gram-negative and Gram-positive bacteria, including antibiotic-resistant strains of both types of bacteria. When used alone or in conjunction with other antibacterial medications, AgNPs have a wide variety of modes of action against diverse bacterial pathogens, such as *E. coli* and *S. aureus*.[43] Since only a small amount of AgNPs were used in this experiment, novel AgNP combinations can be sought for use in this therapeutic approach, which has the potential to reduce tumor burden and prevent infectious diseases, making it a very flexible platform for continuing to fight MDR bacteria. Most antibiotics kill bacteria by altering membrane permeability, synthesis, transcription, translation, and replication enzymatic pathways.[44] Target gene mutation lowers antibiotic-target enzyme binding affinity. Metallic nanoparticles, which have a high surface-to-volume ratio, can treat drug-resistant bacterial infections.[9] Lipopolysaccharide or teichoic acid can enhance membrane attraction to NPs' positive charge. AgNPs destroy bacteria in different manners, rendering resistance unlikely as a result of their different properties, such as shape and size.[9,45,46] Triangular AgNPs, for example, are more efficient against bacteria than spherical or rod-shaped AgNPs because of the increased contact area and molecular binding interactions that result from their smaller size.[47] It has been hypothesized that the colloidal stabilization of AgNPs regulates bacterial signal transduction pathways by changing the phosphotyrosine balance of the proteins, hence inhibiting bacterial growth.[47] When AgNPs enter a bacterial cell, it has the potential to bind to DNA, proteins, and lipids, among other cellular structures and biomolecules. Detrimental effects of AgNPs occur on bacteria when they interact with biological structures and molecules and consequently suppress cell division.[9,29,48]

Conclusion

The burgeoning interest in AgNPs is driven by their versatile properties and potential applications. This research delved into the anti-cancer and antibacterial effects of biogenic AgNPs, harnessed from the airborne fungus *Aspergillus flavus*. The study explored AgNPs' antibacterial activity against Gram-positive and Gram-negative strains, revealing a pronounced impact on *S. aureus*, *S. epidermidis*, *S. enterica*, and *S. typhi* (ATCC 14028). Moreover, the investigation unveiled the potential cytotoxicity of these biogenic particles on MDA-MB-231 breast cancer cells, suggesting that airborne fungal-derived AgNPs possess potent cytotoxic attributes, thus opening avenues for diverse biological utilities. However, there were certain limitations to this study that warrant consideration. Firstly, the low number of tested bacterial strains could introduce bias in the generalizability of results, potentially overlooking strains with varying susceptibilities. Additionally, the exclusive focus on the MDA-MB-231 cancer cell line for cytotoxicity assessment might not fully represent the diverse range of cancer cell responses. Moreover, the absence of *in vivo* models restricts the translation of findings to physiological contexts, and the reliance on single concentrations for cytotoxicity testing could overlook dose-dependent effects. Despite these limitations, the study contributes valuable insights into the potential applications of biogenic AgNPs, warranting further investigations for broader implications.

Conflict of Interest

The authors declare no conflict of interest.

Authors' Declaration

The authors hereby declare that the work presented in this article is original and that any liability for claims relating to the content of this article will be borne by them.

References

1. Naganthran A, Verasoundarapandian G, Khalid FE, Masarudin MJ, Zulkharnain A, Nawawi NM, Karim M, Che Abdullah CA, Ahmad SA. Synthesis, characterization and biomedical application of silver nanoparticles. Materials (Basel). 2022;15(2):427.
2. Khleifat K, Alqaraleh M, Al-limoun M, Alfarrayeh I, Khatib R, Qaralleh H, Alsarayreh A, Al Qaisi Y, Abu Hajleh M. The ability of *Rhizopus stolonifer* MR11 to biosynthesize silver nanoparticles in response to various culture media components and optimization of process parameters required at each stage of biosynthesis. J Ecol Eng. 2022;23(8):89-100. doi:https://doi.org/10.12911/22998993/150673
3. Al-Limoun M, Qaralleh HN, Khleifat KM, Al-Anber M, Al-Tarawneh A, Al-sharafa K, Kailani MH, Zaitoun MA, Matar SA, Al-soub T. Culture media composition and reduction potential optimization of mycelia-free filtrate for the biosynthesis of silver nanoparticles using the fungus *Tritirachium oryzae* W5H. Curr Nanosci. 2020;16(5):757-769.
4. Klaus T, Joerger R, Olsson E, Granqvist CG. Silver-based crystalline nanoparticles, microbially fabricated. Proc Natl Acad Sci. 1999;96(24):13611-13614.
5. Qaralleh H, Khleifat KM, Al-Limoun MO, Alzedaneen FY, Al-Tawarah N. Antibacterial and synergistic effect of biosynthesized silver nanoparticles using the fungi *Tritirachium oryzae* W5H with essential oil of Centaurea damascena to enhance conventional antibiotics activity. Adv Nat Sci Nanosci Nanotechnol. 2019;10(2):25016.
6. Al-Soub A, Khleifat K, Al-Tarawneh A, Al-Limoun M, Alfarrayeh I, Al Sarayreh A, Al Qaisi Y, Qaralleh H, Alqaraleh M, Albashaireh A. Silver nanoparticles biosynthesis using an airborne fungal isolate, *Aspergillus flavus*: optimization, characterization and antibacterial activity. Iran J Microbiol. 2022;14(4):518-528.
7. Khleifat K, Qaralleh H, Al-Limoun M. Antibacterial Activity of Silver Nanoparticles Synthesized by *Aspergillus flavus* and its Synergistic Effect with Antibiotics. J Pure Appl Microbiol. (2022); 16(3):1722-1735. doi: 10.22207/JPAM.16.3.13
8. Khleifat KM. Biodegradation of phenol by *Actinobacillus* sp.: Mathematical interpretation and effect of some growth conditions. *Bioremediat J*. 2007;11(3):103-112.
9. Singh A, Gautam PK, Verma A, Singh V, Shivapriya PM, Shivalkar S, Sahoo AK, Samanta SK. Green synthesis of metallic nanoparticles as effective alternatives to treat antibiotics resistant bacterial infections: A review. Biotechnol Reports. 2020;25:e00427.
10. Khleifat KM, Abboud MM, Al-Mustafa AH, Al-Sharafa KY. Effects of carbon source and Vitreoscilla hemoglobin (VHb) on the production of β-galactosidase in Enterobacter aerogenes. Curr Microbiol. 2006; 53:277-81.
11. Abboud, M. M., Aljundi, I. H., Khleifat, K. M., and Dmour, S. Biodegradation kinetics and modeling of whey lactose by bacterial hemoglobin VHb-expressing Escherichia coli strain. Biochem Eng J. 2010; 48(2): 166-172.
12. Gurunathan S, Qasim M, Park C, Yoo H, Kim JH, Hong K. Cytotoxic potential and molecular pathway analysis of

silver nanoparticles in human colon cancer cells HCT116. Int J Mol Sci. 2018;19(8):2269.
13. Oves M, Rauf MA, Aslam M, Qari HA, Sonbol H, Ahmad I, Zaman GS, Saeed M. Green synthesis of silver nanoparticles by *Conocarpus Lancifolius* plant extract and their antimicrobial and anticancer activities. Saudi J Biol Sci. 2022;29(1):460-471.
14. Patil SB, Hublikar L V, Raghavendra N, Shanbhog C, Kamble A. Synthesis and exploration of anticancer activity of silver nanoparticles using *Pandanus amaryllifolius* Roxb. leaf extract: Promising approach against lung cancer and breast cancer cell lines. Biologia (Bratisl). 2021;76:3533-3545.
15. Lin J, Huang Z, Wu H, Zhou W, Jin P, Wei P, Zhang Y, Zheng F, Zhang J, Xu J. Inhibition of autophagy enhances the anticancer activity of silver nanoparticles. Autophagy. 2014;10(11):2006-2020.
16. Khleifat KM, Matar SA, Jaafreh M, Qaralleh H, Al-limoun MO, Alsharafa KY. Essential oil of *Centaurea damascena* aerial parts, antibacterial and synergistic effect. J Essent Oil Bear Plants. 2019;22(2):356-367.
17. Gurunathan S, Kalishwaralal K, Vaidyanathan R, Venkataraman D, Pandian SRK, Muniyandi J, Hariharan N, Eom SH. Biosynthesis, purification and characterization of silver nanoparticles using *Escherichia coli*. Colloids Surfaces B Biointerfaces. 2009;74(1):328-335.
18. Khlaifat AM, Al-limoun MO, Khleifat KM, Al Tarawneh AA, Qaralleh H, Rayyan EA, Alsharafa KY. Antibacterial synergy of *Tritirachium oryzae*-produced silver nanoparticles with different antibiotics and essential oils derived from *Cupressus sempervirens* and *Asteriscus graveolens* (Forssk). Trop J Pharm Res. 2019;18(12):2605-2616.
19. Khleifat K, Abboud MM. Correlation between bacterial haemoglobin gene (vgb) and aeration: their effect on the growth and α-amylase activity in transformed *Enterobacter aerogenes*. J Appl Microbiol. 2003;94(6):1052-1058.
20. Al-Tawarah NM, Qaralleh H, Khlaifat AM, Nofal MN, Alqaraleh M, Khleifat KM, Al-limoun MO, Al Shhab MA. Anticancer and antibacterial properties of *Verthemia iphionides* essential oil/silver nanoparticles. Biomed Pharmacol J. 2020;13(3):1175-1185.
21. Karna SKL, Ahamad F, Faruq O, Pokharel YR. L-Nω-Nitroarginine Inhibits the Induction of Nitric Oxide Synthase (iNOS) and Cyclooxygenase-2 (COX-2) by Inhibiting NF-κB and AP-1 Activation in RAW 264.7 Cells. Drug Des. 2016;5(135):138-2169.
22. Balint K, Xiao M, Pinnix CC, Soma A, Veres I, Juhasz I, Brown EJ, Capobianco AJ, Herlyn M, Liu ZJ. Activation of Notch1 signaling is required for β-catenin–mediated human primary melanoma progression. J Clin Invest. 2005;115(11):3166-3176.
23. Alqaraleh M, Khleifat KM, Abu Hajleh MN, Farah HS, Ahmed KAA. Fungal-Mediated Silver Nanoparticle and Biochar Synergy against Colorectal Cancer Cells and Pathogenic Bacteria. Antibiotics. 2023;12(3):597.
24. Obeidat NM, Zihlif MA, Alqudah DA, Alshaer W, Alqaraleh M, Abdalla SS. Effects of cyclic acute and chronic hypoxia on the expression levels of metabolism related genes in a pancreatic cancer cell line. Biomed Reports. 2022;17(4):1-11.
25. Pfaffl MW. A new mathematical model for relative quantification in real-time RT–PCR. Nucleic Acids Res. 2001;29(9):e45-e45.
26. Khleifat K, Tarawneh K, Ali Wedyan M, Al-Tarawneh A, Al Sharafa K. Growth kinetics and toxicity of *Enterobacter cloacae* grown on linear alkylbenzene sulfonate as sole carbon source. Curr Microbiol. 2008;57(4):364-370. doi:https://doi.org/10.1007/s00284-008-9203-z
27. Khleifat KM, Sharaf EF, Al-limoun MO. Biodegradation of 2-chlorobenzoic acid by *Enterobacter cloacae*: Growth kinetics and effect of growth conditions. Bioremediat J. 2015;19(3):207-217. doi:https://doi.org/10.1080/10889868.2015.1029113
28. Wypij M, Jędrzejewski T, Trzcińska-Wencel J, Ostrowski M, Rai M, Golińska P. Green synthesized silver nanoparticles: antibacterial and anticancer activities, biocompatibility, and analyses of surface-attached proteins. Front Microbiol. 2021;12:632505.
29. Alfarrayeh I, Tarawneh K, Almajali D, Al-Awaida W. Evaluation of the Antibacterial and Antioxidant properties of the Methanolic extracts of four Medicinal plants selected from Wadi Al-Karak, Jordan related to their Phenolic contents. Res J Pharm Technol. 2022;15(5):2110-2116. doi:https://doi.org/10.52711/0974-360X.2022.00350
30. Al-Sammarraie ON, Alsharafa KY, Al-Limoun MO, Khleifat KM, Al-Sarayreh SA, Al-Shuneigat JM, Kalaji HM. Effect of various abiotic stressors on some biochemical indices of *Lepidium sativum* plants. Sci Rep. 2020;10(1):1-10.
31. Alfarrayeh I, Pollák E, Czéh Á, Vida A, Das S, Papp G. Antifungal and Anti-Biofilm Effects of Caffeic Acid Phenethyl Ester on Different *Candida* Species. Antibiotics. 2021;10(11):1359-1374. doi:https://doi.org/10.3390/antibiotics10111359
32. AshaRani P V, Low Kah Mun G, Hande MP, Valiyaveettil S. Cytotoxicity and genotoxicity of silver nanoparticles in human cells. ACS Nano. 2009;3(2):279-290.
33. Gurunathan S, Han JW, Eppakayala V, Jeyaraj M, Kim JH. Cytotoxicity of biologically synthesized silver nanoparticles in MDA-MB-231 human breast cancer cells. Biomed Res Int. 2013;2013.
34. Park MVDZ, Neigh AM, Vermeulen JP, de la Fonteyne LJJ, Verharen HW, Briedé JJ, van Loveren H, de Jong WH. The effect of particle size on the cytotoxicity, inflammation, developmental toxicity and genotoxicity of silver nanoparticles. Biomaterials. 2011;32(36):9810-9817.
35. Franco-Molina MA, Mendoza-Gamboa E, Sierra-Rivera CA, Gómez-Flores RA, Zapata-Benavides P, Castillo-Tello P, Alcocer-González JM, Miranda-Hernández DF, Tamez-Guerra RS, Rodríguez-Padilla C. Antitumor activity of colloidal silver on MCF-7 human breast cancer cells. J Exp Clin Cancer Res. 2010;29(1):1-7.
36. Gianinazzi C, Grandgirard D, Imboden H, Egger L, Meli DN, Bifrare YD, Joss PC, Täuber MG, Borner C, Leib SL. Caspase-3 mediates hippocampal apoptosis in pneumococcal meningitis. Acta Neuropathol. 2003;105:499-507.
37. Ahmed ST, Ivashkiv LB. Inhibition of IL-6 and IL-10 signaling and Stat activation by inflammatory and stress pathways. J Immunol. 2000;165(9):5227-5237.
38. Yang L, Guo P, Wang P, Wang W, Liu J. IL-6/ERK signaling pathway participates in type I IFN-programmed, unconventional M2-like macrophage polarization. Sci Rep. 2023;13(1):1827.
39. Karin M, Lawrence T, Nizet V. Innate immunity gone awry: linking microbial infections to chronic inflammation and cancer. Cell. 2006;124(4):823-835.
40. Guan K, Zheng Z, Song T, He X, Xu C, Zhang Y, Ma S, Wang Y, Xu Q, Cao Y. MAVS regulates apoptotic cell death by decreasing K48-linked ubiquitination of voltage-dependent anion channel 1. Mol Cell Biol. 2013;33(16):3137-3149.
41. Khleifat KM, Abboud MM, Al-Mustafa AH. Effect of Vitreoscilla hemoglobin gene (vgb) and metabolic inhibitors on cadmium uptake by the heterologous host Enterobacter aerogenes. Process Biochem. 2006;41(4):930-4.
42. Wei LH, Kuo ML, Chen CA, Chou CH, Cheng WF, Chang MC, Su JL, Hsieh CY. The anti-apoptotic role of interleukin-6 in human cervical cancer is mediated by up-

regulation of Mcl-1 through a PI 3-K/Akt pathway. Oncogene. 2001;20(41):5799-5809.
43. Bruna T, Maldonado-Bravo F, Jara P, Caro N. Silver nanoparticles and their antibacterial applications. Int J Mol Sci. 2021;22(13):7202.
44. Khleifat, K. M., Abboud, M. M., Omar, S., & Al-Kurishy, J. H. Urinary tract infection in South Jordanian population. J Med Sci; 2006; 6(1), 5-11.
45. Pal S, Tak YK, Song JM. Does the antibacterial activity of silver nanoparticles depend on the shape of the nanoparticle? A study of the gram-negative bacterium *Escherichia coli*. Appl Environ Microbiol. 2007;73(6):1712-1720.
46. Acharya D, Singha KM, Pandey P, Mohanta B, Rajkumari J, Singha LP. Shape dependent physical mutilation and lethal effects of silver nanoparticles on bacteria. Sci Rep. 2018;8(1):201.
47. Khleifat K, Homady MH, Tarawneh KA, Shakhanbeh J. Effect of Ferula hormonis extract on social aggression, fertility and some physiological parameters in prepubertal male mice. Endocrine J. 2001;48(4):473-82.
48. Markowska K, Grudniak A, Wolska K. Silver nanoparticles as an alternative strategy against bacterial biofilms. Acta Biochim Pol. 2013;60(4):523-530.
49. Kobayashi S, Shimamura T, Monti S, Steidl U, Hetherington CJ, Lowell AM, Golub T, Meyerson M, Tenen DG, Shapiro GI. Transcriptional profiling identifies cyclin D1 as a critical downstream effector of mutant epidermal growth factor receptor signaling. Cancer Res. 2006;66(23):11389-11398.
50. Novakovic P, Stempak JM, Sohn KJ, Kim YI. Effects of folate deficiency on gene expression in the apoptosis and cancer pathways in colon cancer cells. Carcinogenesis. 2006;27(5):916-924.\
51. Al Qaisi YT, Khleifat KM, Alfarrayeh II, Alsarayreh AZ. In Vivo Therapeutic Effect of Some Medicinal Plants' Methanolic Extracts on the Growth and Development of Secondary Hydatid Cyst Infection. Acta Parasitol. 2022;67(4):1521-1534. doi:https://doi.org/10.1007/s11686-022-00605-6